Molecular Biology of the Cell
Vol. 8, 2171–2185, November 1997

Distinct Molecular Events during Secretory Granule Biogenesis Revealed by Sensitivities to Brefeldin A

Carlos J. Fernandez,* Michael Haugwitz, Benjamin Eaton, and Hsiao-Ping H. Moore†

Department of Molecular and Cell Biology, University of California, Berkeley, California 94720-3200

Submitted June 5, 1996; Accepted August 18, 1997
Monitoring Editor: Ari Helenius

The biogenesis of peptide hormone secretory granules involves a series of sorting, modification, and trafficking steps that initiate in the *trans*-Golgi and *trans*-Golgi network (TGN). To investigate their temporal order and interrelationships, we have developed a pulse–chase protocol that follows the synthesis and packaging of a sulfated hormone, pro-opiomelanocortin (POMC). In AtT-20 cells, sulfate is incorporated into POMC predominantly on N-linked endoglycosidase H-resistant oligosaccharides. Subcellular fractionation and pharmacological studies confirm that this sulfation occurs at the *trans*-Golgi/TGN. Subsequent to sulfation, POMC undergoes a number of molecular events before final storage in dense-core granules. The first step involves the transfer of POMC from the sulfation compartment to a processing compartment (immature secretory granules, ISGs): Inhibiting export of pulse-labeled POMC by brefeldin A (BFA) or a 20°C block prevents its proteolytic conversion to mature adrenocorticotropic hormone. Proteolytic cleavage products were found in vesicular fractions corresponding to ISGs, suggesting that the processing machinery is not appreciably activated until POMC exits the sulfation compartment. A large portion of the labeled hormone is secreted from ISGs as incompletely processed intermediates. This unregulated secretory process occurs only during a limited time window: Granules that have matured for 2 to 3 h exhibit very little unregulated release, as evidenced by the efficient storage of the 15-kDa N-terminal fragment that is generated by a relatively late cleavage event within the maturing granule. The second step of granule biogenesis thus involves two maturation events: proteolytic activation of POMC in ISGs and a transition of the organelle from a state of high unregulated release to one that favors intracellular storage. By using BFA, we show that the two processes occurring in ISGs may be uncoupled: although the unregulated secretion from ISGs is impaired by BFA, proteolytic processing of POMC within this organelle proceeds unaffected. The finding that BFA impairs constitutive secretion from both the TGN and ISGs also suggests that these secretory processes may be related in mechanism. Finally, our data indicate that the unusually high levels of unregulated secretion often associated with endocrine tumors may result, at least in part, from inefficient storage of secretory products at the level of ISGs.

INTRODUCTION

Newly synthesized peptide hormones traverse the secretory pathway until the *trans*-Golgi network (TGN),[1] where they are packaged into nascent secretory vesicles that mature into regulated granules (reviewed in Burgess and Kelly, 1987; Bauerfeind and Huttner, 1993; Moore *et al.*, 1993). Bioactive peptides are gener-

* Present address: Cell Biology Laboratory, Imperial Cancer Research Fund, London WC2A 3PX, United Kingdom.
† Corresponding author: Department of Molecular and Cell Biology, University of California at Berkeley, 142 Life Sciences Addition No. 3200, Berkeley, CA 94720-3200.

[1] Abbreviations used: ACTH, adrenocorticotropic hormone; BFA, brefeldin A; CPC, cetylpyridinium chloride; ER, endoplasmic reticulum; GAG, glycosaminoglycan; IAA, iodoacetamide; ISG, immature secretory granule; PMSF, phenylmethylsulfonyl fluoride; PNS, postnuclear supernatant; POMC, pro-opiomelanocortin; TGN, *trans*-Golgi network; TCA, trichloroacetic acid.

© 1997 by The American Society for Cell Biology

ated from prohormones by proteolytic cleavage at paired basic residues (reviewed in Hutton, 1990; Lindberg, 1991; Steiner *et al.*, 1992; Seidah *et al.*, 1993). The exact compartment in which processing takes place appears to depend on the individual peptide hormone, although in general, it is a relatively late event occurring in the TGN or maturing secretory granules (Tooze *et al.*, 1987a; Davidson *et al.*, 1988; Schnabel *et al.*, 1989; Huang and Arvan, 1994; Orci *et al.*, 1994; Xu and Shields, 1994). In some cases, the lumenal pH of these compartments has been shown to play a direct role in activating propeptide processing (for example, see Schmidt and Moore, 1995; Anderson *et al.*, 1997).

Sorting of constitutive secretory proteins from regulated secretory proteins was first shown to occur in the TGN (Orci *et al.*, 1987; Tooze *et al.*, 1987b; Tooze and Huttner, 1990), but more recent studies suggest that it continues in immature secretory granules (ISGs). This argument is based on the following findings: 1) Kinetic analysis of secretion in parotid cells indicates that constitutive secretion from this cell type occurs almost entirely after the pulse-labeled secretory proteins have appeared in newly formed granules (von Zastrow and Castle, 1987), 2) pulse–chase experiments in islet β-cells demonstrate that the C-peptide of insulin is preferentially secreted from ISGs in an unregulated manner (Kuliawat and Arvan, 1992), and 3) ISGs isolated from PC-12 cells contain more constitutive proteins than mature granules do, suggesting that continual sorting must occur as the granules mature (Grimes and Kelly, 1992). Sorting is thought to be accomplished by budding of "constitutive-like vesicles" from ISGs (Kuliawat and Arvan, 1992). In addition, ISGs probably undergo other budding and fusion events during maturation. Electron microscopic, physiological, and cell biological studies suggest that ISGs may fuse with each other (Kalina *et al.*, 1988; de Toledo and Fernandez, 1990; Tooze *et al.*, 1991; Lew *et al.*, 1994). Excess membranes may then be removed from the fused granules by vesicle budding, resulting in an increase in granule density. Recent data suggest that ISGs may bud off vesicles destined for endosomes/lysosomes (Kuliawat and Arvan, 1994). At present, the mechanism for ISG maturation is poorly understood. It is unclear how many vesicle budding and/or fusion steps are required and whether any of these steps are interrelated. For instance, it is not known whether budding of constitutive-like vesicles contributes to the change in buoyant density and/or acidity of ISGs. In the endosomal system, vesicle-mediated removal of Na^+-K^+-ATPase from the early endosomes is believed to allow further acidification of the late endosomes (Cain *et al.*, 1989; Fuchs *et al.*, 1989). Budding of constitutive-like vesicles from ISGs could involve a mechanism similar to budding of constitutive vesicles from the TGN. Alternatively, the two budding processes may employ completely different mechanisms.

In this study, we employed the mouse anterior pituitary cell line AtT-20 to study these questions. AtT-20 cells have been used extensively as a model system to study vesicular traffic, sorting, targeting, and processing of peptide hormones (Mains and Eipper, 1978; Moore *et al.*, 1983b; Tooze *et al.*, 1987b; Thomas *et al.*, 1991; Ngsee *et al.*, 1993). We took advantage of the finding that pro-opiomelanocortin (POMC) is sulfated in AtT-20 cells and developed a labeling protocol suitable for pulse–chase experiments to study the interrelationship of events occurring in granule biogenesis. We have found that brefeldin A (BFA) inhibits constitutive secretion from the TGN and blocks the transfer of POMC from the site of sulfation to the site of processing. At the level of ISGs, BFA impairs the unregulated release from this organelle. These results suggest that constitutive secretion from the TGN and the process of unregulated release from ISGs may involve a similar BFA-sensitive mechanism. By contrast, BFA has no effect on the proteolytic activation of prohormone within ISGs. The density increase of secretory granules resulting from condensation is also not significantly affected by BFA. These results suggest that γ-adaptin and clathrin, which have been shown to be recruited by ISGs in a BFA-sensitive manner (Dittie *et al.*, 1996), do not play a major role in regulating prohormone processing and condensation within this organelle.

Another important issue concerns the molecular defects associated with secretory granule biogenesis in endocrine tumors. Targeting of peptide hormones to dense-core granules of endocrine tissues in vivo occurs efficiently (Rhodes and Halban, 1987; Carroll *et al.*, 1988; Kuliawat and Arvan, 1992). By contrast, tumor endocrine cell lines often secrete a large amount of hormones in an unregulated manner (Gumbiner and Kelly, 1982; Moore *et al.*, 1983a; Reaves *et al.*, 1990), which may explain the elevated serum levels of hormones associated with many endocrine tumors (Modlin *et al.*, 1993; Meko and Norton, 1995; Orth, 1995). The molecular basis for this defect is unknown. It could, in principle, be due to defective sorting in the TGN, defective retention at the level of ISGs, or other defects associated with mature secretory granules. We provide evidence to show that a major secretion defect in the AtT-20 tumor cell line lies in inefficient storage of hormone products at the level of ISGs.

MATERIALS AND METHODS

Antisera and Reagents

Affinity-purified rabbit anti-porcine adrenocorticotropic hormone (ACTH) was prepared as described (Moore and Kelly, 1985). It recognizes POMC as well as all peptides containing residues 1–39 of mature ACTH (Figure 1). BFA was purchased from Boehringer Mannheim (Indianapolis, IN), monensin was from Fluka (Ronkonkoma, NY), tunicamycin was from Sigma (St. Louis, MO), endoglycosidase H (endo H) was from Boehringer Mannheim (In-

dianapolis, IN), and endo F was from New England Biolabs (Beverley, MA).

Cell Culture and Pulse–Chase Experiments

AtT-20 cells were maintained in DMEM (BioWhittaker, Walkersville, MD) supplemented with 10% fetal calf serum under 15% CO_2 at 37°C. For radiolabeling experiments, cells were seeded at a density of 2×10^5 cells/well in a 12-well dish (Corning, Oneonta, NY) and grown for 36 to 48 h. For sulfate labeling, the cells were preincubated for 30 min at 37°C in buffer A [110 mM NaCl, 5.4 mM KCl, 0.9 mM Na_2HPO_4, 10 mM $MgCl_2$, 2 mM $CaCl_2$, 1 g/l glucose, 20 mM *N*-(2-hydroxyethyl)piperazine-*N*′-(2-ethanesulfonic acid) (HEPES), pH 7.2]. The cells were then labeled with 150–200 μl of 1–2.5 mCi/ml [^{35}S]sulfate (ICN, Costa Mesa, CA) in buffer A. Drug treatments and chases were all performed in DMEM. Methionine labeling was performed as described (Moore *et al*, 1983a). Medium samples were collected and cleared of cell debris by centrifugation (15,000 × *g*, 5 min); iodoacetamide (IAA) and phenylmethylsulfonyl fluoride (PMSF) were added to a final concentration of 0.3 mg/ml. To recover ACTH-containing peptides by immunoprecipitation, the cells were extracted with ice-cold NDET [1% Nonidet P-40, 0.4% deoxycholate, 66 mM EDTA, 10 mM Tris(hydroxymethyl)aminomethane, pH 7.4] containing IAA and PMSF. Insoluble materials were removed by centrifugation (15,000 × *g*, 10 min), and the supernatants from cell extracts and medium were used for immunoprecipitation. To analyze all sulfated products (see Figure 5), pulse-labeled cells were washed and incubated in DMEM supplemented with bovine serum albumin to a final concentration of 20 μg/ml at 37°C for indicated chase times. Secretion medium was collected, cleared of debris, and then precipitated with trichloroacetic acid (TCA; final concentration, 20%) for 1 h on ice followed by centrifugation in a Microfuge at 15,000 × *g* for 15 min at 4°C. Pellets were washed once with acetone before loading on the gels. Cells were harvested with 0.7% Triton X-100, 25 mM HEPES, pH 7.2, PMSF, IAA, and the insoluble materials was removed by centrifugation as above. The cell extracts were either precipitated with TCA as above (see Figure 5B) or precipitated with 4 times the volume of ice-cold acetone (see Figure 5A). Acetone precipitates were collected by centrifugation at 2500 × *g* for 1 h at 4°C and analyzed by SDS-PAGE.

An epitope-tagged human Rab 11 vector was constructed as described (Chen *et al.*, 1993), and a stable clone of AtT-20 cells was isolated according to Chavez *et al.* (1994).

Secretion of glycosaminoglycan (GAG) Chains

Cells grown in 12-well plates were incubated in sulfate-free DMEM containing 0.5 mM 4-methylumbelliferyl β-D-xyloside (xyloside; Sigma) for 30 min and then radiolabeled with 150 μCi/ml [^{35}S]sulfate (ICN Biochemicals) for 5 min. Cells from one well were extracted to determine the amount of total label incorporated, and the remainders were chased in the presence or absence of 5 μg/ml BFA. Medium samples were collected after each chase and the cells were extracted at the end of the chases. Samples were processed for cetylpyridinium chloride (CPC) assays of GAG chains as described (Miller and Moore, 1992).

Immunoprecipitation and Immunoblotting

POMC products were isolated from sulfate-labeled samples by single immunoprecipitation (Moore and Kelly, 1985) and from methionine-labeled samples by a double immunoprecipitation procedure (Moore and Kelly, 1986). Where indicated, immune precipitates were eluted from staphylococcus A with 0.5% SDS, 1% 2-mercaptoethanol and one-half of each sample was incubated with endo H in 50 mM sodium citrate, pH 5, for 12 to 16 h at 37°C or endo F in 24 mM Na_2HPO_4, pH 7.4, 10 mM EDTA, 0.5% Triton X-100 for 1 h at 37°C. Immunoprecipitates were subjected to reducing SDS-PAGE and exposed for 48 to 72 h to a PhosphorImager cassette (Molecular Dynamics, Sunnyvale, CA). For immunoblot of rab11, transfected AtT-20 cells were fractionated as described below, and proteins from each fraction were precipitated with TCA. The precipitates were subjected to SDS-PAGE and transferred onto nitrocellulose (Schleicher and Schuell, Keene, NH). The blot was probed with the monoclonal antibody 12CA5 (BABCO, Berkeley, CA) against hem-

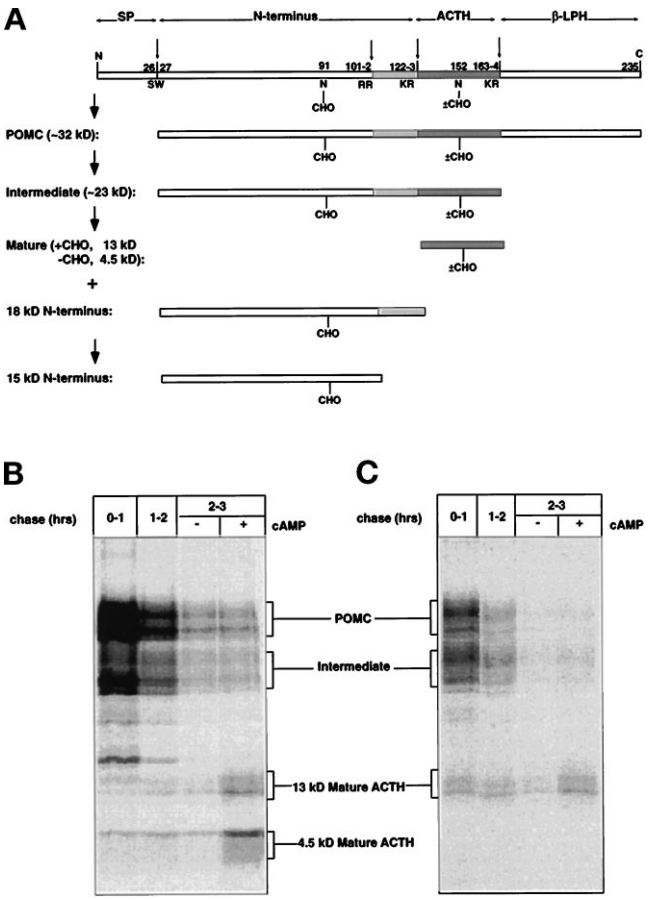

Figure 1. Subset of POMC-derived peptides secreted from AtT-20 cells can be labeled with [^{35}S]sulfate. (A) Domain structure of POMC relevant to this study, showing N-linked glycosylation (CHO) sites and the temporal order of proteolytic cleavages at pairs of basic residues. Dark-shaded portion indicates the mature ACTH peptide against which antibodies used in this study were raised. Only POMC peptides that contain the major sulfation sites are shown. SP, signal peptide; ±CHO, the glycosylation site is not always used. ACTH-containing peptides secreted from [^{35}S]methionine-labeled cells (B) and from [^{35}S]sulfate labeled cells (C). Identical cultures of AtT-20 cells were labeled with [^{35}S]methionine for 15 min or [^{35}S]sulfate for 5 min. The cells were then chased in unlabeled DMEM for three consecutive 1-h periods. During the last hour of chase, 8-Br-cAMP was added to one well to stimulate release from mature regulated secretory granules. A parallel culture was chased in medium lacking 8-Br-cAMP as control. Chase medium was collected, ACTH-related peptides were immunoprecipitated with affinity-purified anti-ACTH, and radiolabeled bands in the immunoprecipitates were separated by SDS-PAGE on 18% gels and analyzed by PhosphorImager.

agglutinin and analyzed by the chemiluminescence method (ECL, Amersham, Arlington Heights, IL).

Subcellular Fractionation of Sulfated POMC Products

Equilibrium Centrifugation. The D_2O-Ficoll gradient procedure of Chavez *et al.* (1994) was used to isolate mature secretory granules (Figure 3). Alternatively, a D_2O-sucrose gradient was used (see Figure 9). Cells in 15-cm dishes were homogenized (1 ml/dish), and a postnuclear supernatant (PNS) was prepared by centrifugation for 10 min at 1000 × *g*. Four hundred microliters of PNS were loaded onto a step gradient containing 1-ml steps of 50, 30, 27.5, 25, 22.5, 20, 17.5, 15, 12.5, and 10% sucrose, all in D_2O buffered with 10 mM HEPES, pH 7.4. The gradient was centrifuged for 3 h at 36,000 rpm at 4°C in a SW41 rotor. One-milliliter fractions were collected from the bottom. Labeled POMC products in each fraction were analyzed as above. Labeled POMC products were detected by solubilizing each fraction with NDET buffer and immunoprecipitation with anti-ACTH.

Velocity Centrifugation. The velocity gradient procedure of Tooze and Huttner (1990) was employed to separate ISGs from *trans*-Golgi/TGN (see Figure 6). Sulfate-labeled cells in a 15-cm dish were lifted by incubating with Ca^{2+}/Mg^{2+}-free PBS containing 1 mM EDTA and collected by centrifugation at 800 rpm in a GPR centrifuge (Beckman, Palo Alto, CA). Cell pellets were washed once in iced homogenization buffer (1 mM EDTA, 1 mM magnesium acetate, 1.6 mM Na_2SO_4, 250 mM sucrose, 10 mM HEPES, pH 7.15, PMSF, IAA), and resuspended in 0.7–0.8 ml of iced homogenization buffer. The resuspended cells were passed through a 20-gauge needle and then homogenized by using an EMBL homogenizer. The homogenate was centrifuged (10 min 1000 × *g*) and the resulting postnuclear supernatant was loaded onto a linear 0.3–1.2 M sucrose gradient prepared in homogenization buffer. The gradients were centrifuged for 15 min at 25,000 rpm in a Beckman SW 41 Ti rotor at 4°C. The load volume was discarded and 0.8-ml fractions were collected. The fractions were diluted with water to 1 ml and precipitated with 4 ml of acetone at −20°C for 1 h, and the precipitates were collected by centrifugation in a Beckman GPR centrifuge at 3500 rpm for 1 h.

RESULTS

[^{35}S]Sulfate Is Incorporated into a Subset of POMC-derived Peptides in AtT-20 Cells

Previous trafficking studies have used methionine or cysteine labeling of AtT-20 cells. In this study, we have developed a pulse–chase protocol taking advantage of the fact that POMC is sulfated (Hoshina *et al.*, 1982; Moore *et al.*, 1983). Because sulfation usually occurs in the Golgi or TGN, labeling with [^{35}S]sulfate allows a more precise kinetic analysis of the post-Golgi events. We first compared POMC products labeled with [^{35}S]methionine or [^{35}S]sulfate (Figure 1). Pulse-labeled cells were chased for 2 h and then stimulated with 8-Br-cAMP to trigger secretion from the regulated pathway. ACTH-related peptides were immunoprecipitated from the chase medium with affinity-purified antibodies recognizing epitopes on mature ACTH (residues 1–39; Figure 1A). [^{35}S]Methionine-labeled cells secreted a number of peptides in an unregulated manner (Figure 1B): a doublet of 30–35 kDa corresponding to singly and doubly glycosylated POMC precursors, and bands of 20–25 kDa corresponding to intermediates generated by the first endoproteolytic cleavage at ACTH-β-Lipotropin junction (Figure 1A). 8-Br-cAMP stimulated the secretion of two processed peptides corresponding to 13-kDa glycosylated mature ACTH and 4.5-kDa unglycosylated mature ACTH (Figure 1B). [^{35}S]Sulfate labeling of cells produced a similar pattern (Figure 1C), with a notable exception that the unglycosylated 4.5-kDa ACTH was not labeled. Thus, [^{35}S]sulfate may be used to specifically label a subset of POMC peptides. Targeting of POMC peptides to the regulated pathway does not appear to depend on their states of sulfation.

POMC Is Sulfated Predominantly on N-linked Oligosaccharides in the trans-Golgi/TGN

Because 13-kDa and 4.5-kDa ACTH differ only in N-linked glycosylation on Asn^{152} (Figure 1A), we tested whether sulfate is incorporated into POMC on N-linked carbohydrates. Cells were pretreated with tunicamycin and then labeled with either [^{35}S]sulfate or [^{35}S]methionine (Figure 2). Tunicamycin caused [^{35}S]methionine-labeled POMC doublet to collapse into a single unglycosylated form without significantly affecting the amount of methionine incorporation (Figure 2, compare lanes 1 and 3). The same treatment caused [^{35}S]sulfate-labeled POMC to collapse into a similar band, but the amount of sulfate incorporated was reduced by more than 90% (Figure 2, compare lanes 5 and 7). In a separate experiment, we show that endo F treatment of [^{35}S]sulfate-labeled POMC decreased the recovery of radioactivity to below detection levels (Figure 2, lanes 9 and 10). Thus, the majority of sulfate incorporation on POMC occurs on N-linked carbohydrates.

To determine the intracellular location of POMC sulfation, the above samples were subjected to endo H digestion. POMC labeled in the endoplasmic reticulum (ER) by a [^{35}S]methionine pulse was in the endo H-sensitive form (Figure 2, lanes 1 and 2); the unglycosylated form was not sensitive to endo H as expected (Figure 2, lanes 3 and 4). By contrast, POMC labeled by a 5-min [^{35}S]sulfate pulse was resistant to endo H digestion (Figure 2, lanes 5 and 6), suggesting that sulfation occurs after POMC has reached at least the *medial*-Golgi. To further resolve the site of POMC sulfation, we treated cells with monensin prior to sulfate labeling. Monensin is known to block transport of viral glycoproteins from the *medial*-Golgi to the *trans*-Golgi (Griffiths *et al.*, 1983). If sulfation of POMC occurs at or beyond the *trans*-Golgi, it should greatly reduce sulfate incorporation. Indeed, POMC sulfation was reduced to 20–25% of control levels during a 5- to 60-min pulse (Table 1), suggesting that POMC sulfation occurs after the protein has been delivered to at least the *trans*-Golgi. Treatment with BFA also supported this view: pretreatment of cells with BFA

caused a two- to fivefold reduction in sulfate incorporation into POMC (Table 1). This finding is consistent with the notion that POMC sulfation normally occurs in the TGN and that BFA, by uncoupling the TGN from the Golgi/ER system (Chege and Pfeffer, 1990), prevents POMC from reaching the sulfotransferase compartment. However, the possibility that BFA may exert its effect indirectly by inhibiting sulfotransferase activity could not be excluded in this experiment.

If sulfation indeed occurs in the *trans*-Golgi/TGN, one would expect to find pulse-labeled POMC in a low-density organelle and subsequent chases should result in its transfer to denser compartments. Cells were pulse-labeled with [^{35}S]sulfate, and subcellular organelles were fractionated on a D_2O-Ficoll equilibrium gradient (Chavez *et al*, 1994). As shown in Figure 3, labeled POMC immediately after the pulse was in low-density membranes at the top of this gradient. For comparison, we treated the same cells with a membrane-permeant xyloside to induce synthesis of the constitutive secretory marker, GAG chains (Miller and Moore, 1992): labeled GAG chains after a 5-min pulse were found cofractionating with sulfated POMC. These fractions also contained rab11, a GTPase reported to reside in TGN and post-Golgi vesicles in PC-12 cells (Urbe *et al.*, 1993). By contrast, when cells were labeled for 3 h instead of 5 min, the majority of labeled sulfate was associated with the 13-kDa ACTH found in dense fractions (Figure 3B) that corresponded to mature secretory granules (Chavez *et al.*, 1994); the constitutive marker GAG labeled during the last 30 min was found in light fractions as expected. These data indicate that POMC and GAG chains are sulfated in compartment(s) with density corresponding to *trans*-Golgi/TGN. Within 3 h, the labeled cleavage products are sorted away from constitutively secreted markers and stored in dense organelles.

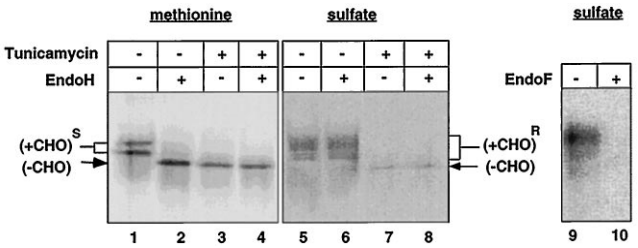

Figure 2. POMC is sulfated primarily on N-linked carbohydrates after the acquisition of endo H resistance. AtT-20 cells were pretreated with 5 μg/ml tunicamycin for 3.5 h and then labeled with [^{35}S]sulfate for 5 min or [^{35}S]methionine for 15 min. The cells were immediately extracted and labeled POMC was immunoprecipitated. One-half of each sample was then subjected to digestion with endo H. Lanes 1–4 are samples from methionine-labeled cells, and lanes 5–8 are from sulfate-labeled cells. For lanes 9 and 10, cells were labeled with [^{35}S]sulfate as in lanes 5 and 6, except that digestion was performed with endo F instead of endo H. CHO^S and CHO^R, endo H-sensitive and endo H-resistant forms, respectively.

Proteolytic Processing of POMC Occurs Predominantly after Its Export from the Sulfation Compartment

Kinetic analysis demonstrated that POMC sulfation precedes proteolytic processing (Figure 4A): a 5-min pulse produced only labeled POMC, but extending the label to 20–60 min resulted in the progressive appearance of labeled intermediate and the 13-kDa mature ACTH. These results were further confirmed by pulse–chase experiments (Figure 4B). The only labeled products after a 5-min pulse labeling were unprocessed POMC. After a 15-min chase at 37°C, a small amount of labeled intermediate began to appear. By the end of a 90-min chase, most of the radiolabel remaining in the cells was proteolytically converted to mature ACTH. The sequential appearance of POMC, intermediates, and then mature ACTH suggests that sulfate is incorporated into POMC, which then gives rise to labeled intermediates and mature ACTH by proteolytic processing. We noticed that the amount of

Table 1. Effects of monensin and BFA pretreatment on [^{35}S]sulfate incorporation into POMC-derived peptides

	Control				Monensin				BFA			
Pulse time (min)	Total incorp. (cpm)	% in POMC	% in interm.	% in mature	Total incorp. (cpm)	% in POMC	% in interm.	% in mature	Total incorp. (cpm)	% in POMC	% in interm.	% in mature
5	1,252	100	0	0	286	100	0	0	402	100	0	0
20	13,270	89	10	1	3,312	100	0	0	2,535	100	0	0
60	9,892	65	28	7	2,006	100	0	0	4,462	100	0	0

AtT-20 cells were pretreated with 10 mM monensin or 5 mg/ml BFA for 45 min before labeling with [^{35}S]sulfate for 5, 20, or 60 min in the presence of the agents. The cells were extracted without further chases, and the total amount of label incorporated (incorp.) into POMC precursors plus intermediates (interm.) plus mature forms was quantitated by using a PhosphorImager. For each condition, the relative amount of individual POMC form was expressed as the percentage of total label incorporated into all forms for that time point.

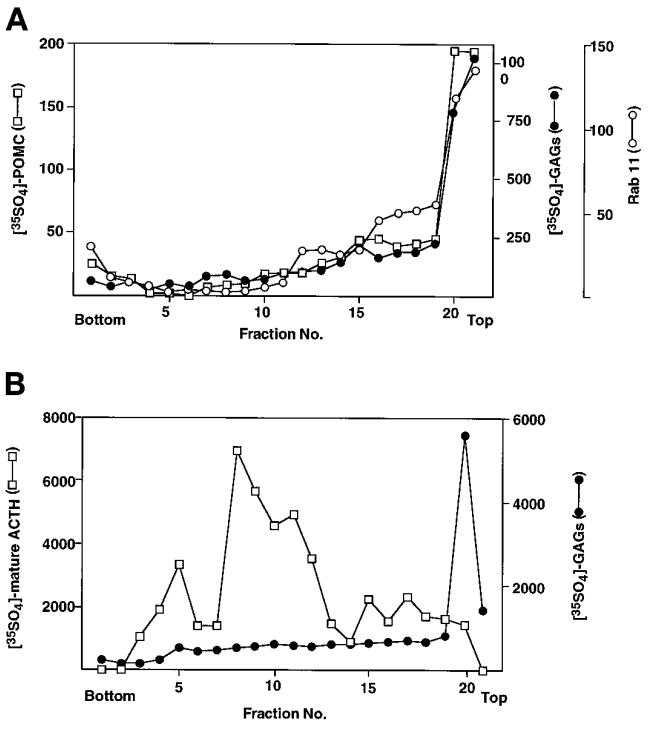

Figure 3. Sulfated POMC products migrate through intracellular compartments with increasing densities. (A) Sulfated POMC was recovered in light-density membranes immediately after pulse labeling. To localize the compartment for sulfation of POMC, AtT-20 cells were labeled with [^{35}S]sulfate for 5 min and homogenized. Membranes from a PNS were fractionated on a D_2O-Ficoll density gradient and labeled POMC products in each fraction were analyzed by SDS-PAGE and PhosphorImager. Under this condition, only unprocessed POMC was recovered. □, Relative amount of sulfate-labeled POMC (in arbitrary scanning units). To localize a constitutive secretory marker on this gradient, AtT-20 cells were treated with xyloside for 30 min and then pulse-labeled with [^{35}S]sulfate for 5 min to label GAG chains. Cells were homogenized and membranes were fractionated as above. The amount of labeled GAG chains in each fraction was assayed by a CPC precipitation/filtration assay. ●, Amount of GAG-associated radioactivity (in cpm) in each fraction. To localize rab 11-containing membranes on the same gradient, AtT-20 cells stably transfected with an influenza hemagglutinin epitope-tagged rab 11 were used, and rab11 immunoreactivity in each fraction was determined by immunoblotting using anti-hemagglutinin antibody. ○, Relative intensity obtained from scanning the Western blot. (B) Cells were continuously labeled with [^{35}S]sulfate for 3 h. Xyloside was added to the cells during the last 30 min to label newly synthesized [^{35}S]GAG chains. Cells were then homogenized and the membranes were fractionated as above. One half of each fraction was assayed for GAG, and the other half was subjected to immunoprecipitation with anti-ACTH. ●, Amount of GAG-associated radioactivity (in cpm) in each fraction; □, distribution of labeled mature ACTH in arbitrary scanning units. Because no chase was performed, a small peak corresponding to newly labeled POMC was also present on the top of this gradient (not shown). POMC, GAG, and rab11 peak at a density of 1.12 g/ml, and mature ACTH peaks at a density of 1.20 g/ml.

cellular radioactivity increased at 0–15 min and then dropped precipitously between 15 and 90 min of chase. The increase is most likely due to a short lag in chasing out the intracellular [^{35}S]sulfate pool. The loss of radiolabel can be attributed to 1) about half of the labeled POMC and intermediates were secreted from the cells (see Figure 1C) and 2) the N-terminal segments carrying a major sulfation site were not recovered in the immune precipitates.

To test whether POMC is processed after sulfation within the same compartment or in a later part of the pathway, we tested the effect of inhibiting TGN export on proteolytic conversion. A manipulation known to block export from the TGN is the 20°C treatment (Matlin and Simons, 1983). Incubation of cells at 20°C for 2 h after a 5-min pulse labeling resulted in little conversion of labeled POMC to mature ACTH (compare Figure 4B, lane 1, to Figure 4C, lanes 1 and 2). Control experiment shows that this inhibition is not due to inactivation of prohormone convertase activity at low temperatures: mature ACTH could be produced at 20°C if labeled POMC was first chased out of the sulfation compartment by a 15-min incubation at 37°C (compare Figure 4B, lane 2, to Figure 4C, lanes 3 and 4). Reduced POMC processing at 20°C is consistent with previous finding using methionine labeling (Milgram and Mains, 1994). Our data suggests the following sequence of events: sulfation of POMC → export → processing to intermediate forms → processing to mature ACTH.

Incompletely Processed POMC Products Are Secreted Constitutively from ISGs during a Limited Time Window

The above analysis suggests that the majority of POMC processing occurs after it exits the sulfation compartment, presumably in ISGs (see below). Because cleaved POMC products were released from the cells in an unregulated manner (see Figure 1), we surmise that constitutive secretion continues to occur after the labeled proteins have reached the ISGs. This process, termed "constitutive-like secretion" from ISGs, has slower kinetics than constitutive secretion from the TGN in other cell types. We therefore examined the time course and composition of the unregulated release of POMC products from AtT-20 cells to determine its origin.

POMC undergoes sequential cleavages, and the pattern of the secreted peptides provides useful information regarding the selectivity and time window of release. In particular, the 18-kDa N-terminal fragment is known to be further cleaved at Arg^{101}–Arg^{102} to give rise to a 15-kDa N-terminal fragment (Cullen and Mains, 1987; see Figure 1). We found that both the 18-kDa and the 15-kDa fragments were labeled with [^{35}S]sulfate and could be followed by simple TCA precipitation (Figure 5). Furthermore, conversion of the 18-kDa to the 15-kDa fragment was a relatively late event that could be blocked at 15°C: if pulse-

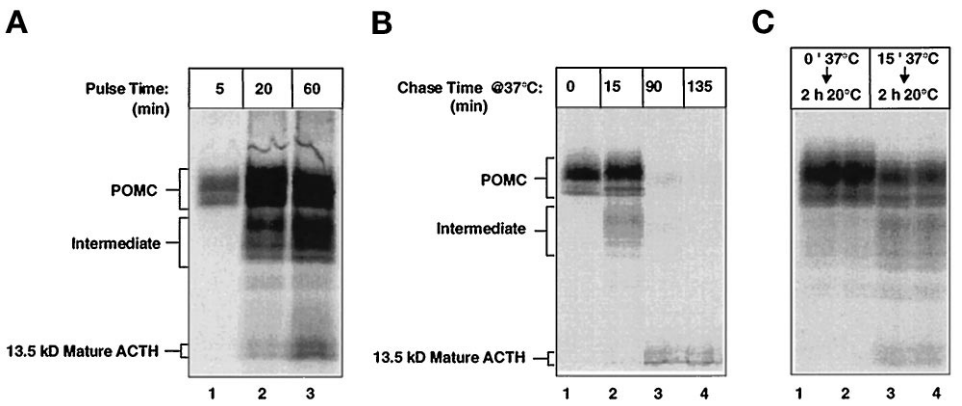

Figure 4. Sulfate incorporation precedes endoproteolytic processing. (A) Continuous labeling. AtT-20 cells were labeled with [^{35}S]sulfate for 5, 20, or 60 min. Cells were extracted with detergent, and the samples were immunoprecipitated with anti-ACTH antibodies. The labeled proteins in the immune precipitates were analyzed by SDS-PAGE and PhosphorImager. (B) Pulse–chase analysis. Cells were pulse-labeled with [^{35}S]sulfate for 5 min and then chased for the times indicated. At the end of each chase, labeled POMC products in the cells were extracted, immunoprecipitated, and analyzed as in A. (C) Effect of a 20°C incubation on proteolytic processing; duplicate samples are shown. Lanes 1 and 2, cells pulse-labeled as in B (lane 1) were shifted to 20°C for 2 h before extraction. Under this condition, little processing occurred during the 20°C incubation period. Lanes 3 and 4, pulse-labeled cells were first chased at 37°C for 15 min as in B (lane 2) before being shifted to 20°C for 2 h. The 15-min chase allowed labeled POMC to exit the sulfation compartment, and subsequent incubation at 20°C resulted in the production of mature ACTH. Thus, processing requires POMC exit from the TGN, and the prohormone convertase is not inactivated at 20°C.

labeled cells were first chased for 15 min at 37°C to allow POMC to exit the sulfation compartment and then incubated at 15°C for 3 h, the 18-kDa N-terminal fragment predominated instead of the 15-kDa N-terminal fragment seen at 37°C (Figure 5A, compare lane 2 to lane 3). To determine whether both the 18-kDa and the 15-kDa N-terminal fragments were released equally from the cells, we monitored the time course of secretion by using TCA precipitation (Figure 5B). The bulk of unregulated release of sulfated products occurred during the first 2–3 h of chase (Figure 5, lanes 1–14). The processed peptides found in the cells were released into the medium with a lag of ~30 min, the first hour being mostly unprocessed POMC and intermediates and the second hour mostly the 18-kDa N-terminal fragment and the 13-kDa ACTH (Figure 5, lanes 9 and 11). Much less release was observed during the third hour of chase (Figure 5, lane 13). A striking difference is that although a significant amount of the 18-kDa N-terminal fragment was secreted, very little of the 15-kDa N-terminal fragment was released into the medium even after prolonged chases (Figure 5, lanes 11–14). Quantitation of the secretion of POMC, the 18-kDa and the 15-kDa N-termini is shown in Figure 5C. To compare these secretion kinetics with that of a constitutive marker, we treated cells with xyloside for 30 min to induce synthesis of the constitutive secretory marker GAG and pulse-labeled them with [^{35}S]sulfate for 5 min. The amount of labeled GAG secreted was determined and plotted in Figure 5C. GAG chains secretion occurred with considerably faster kinetics, reaching a plateau within 1 h of chase. Because significant amounts of POMC intermediates and the 18-kDa N terminus were still secreted after 1 h, we suggest that these processed POMC products were released from ISGs rather than directly from the TGN. Additionally, constitutive-like secretion from ISGs took place only within a limited time window of 2–3 h, after which little additional secretion occurred. This time window coincided with the production of the 15-kDa N-terminal fragment, resulting in its efficient storage in mature granules.

To obtain more direct evidence that ISGs are the major site for POMC processing and for the unregulated release of cleavage products, we employed the velocity gradient procedure of Tooze and Huttner (1990) to separate ISGs from *trans*-Golgi/TGN. Immediately after the pulse labeling, the majority of sulfated POMC was associated with fast-migrating organelles in fractions previously described to correspond to the *trans*-Golgi/TGN (Figure 6A); very little processed forms were detected when the PNS was prepared immediately after the 5-min pulse labeling. By contrast, when pulse-labeled cells were first chased for 15 min at 37°C before preparation for PNS, the majority of label was associated with slower-migrating organelles in fractions corresponding to ISGs (Figure 6B). Notably, some processed intermediate, the 18-kDa N terminus, and the 13-kDa ACTH were also detected in fractions corresponding to ISGs (fractions 12–14) but not the *trans*-Golgi/TGN (fractions 3–7). We noticed that the amount of processing observed in gradient centrifugation experiments were consistently more extensive than in secretion experiments (for example, compare Figure 6B with Figure 5B, lane 4). This discrepancy was observed only from cells that had been chased at 37°C (Figure 6B) but not from pulse-labeled cells (Figure 6A), and our unpublished results indicate that this was due to continued proteolytic cleavage in the processing compartment during ma-

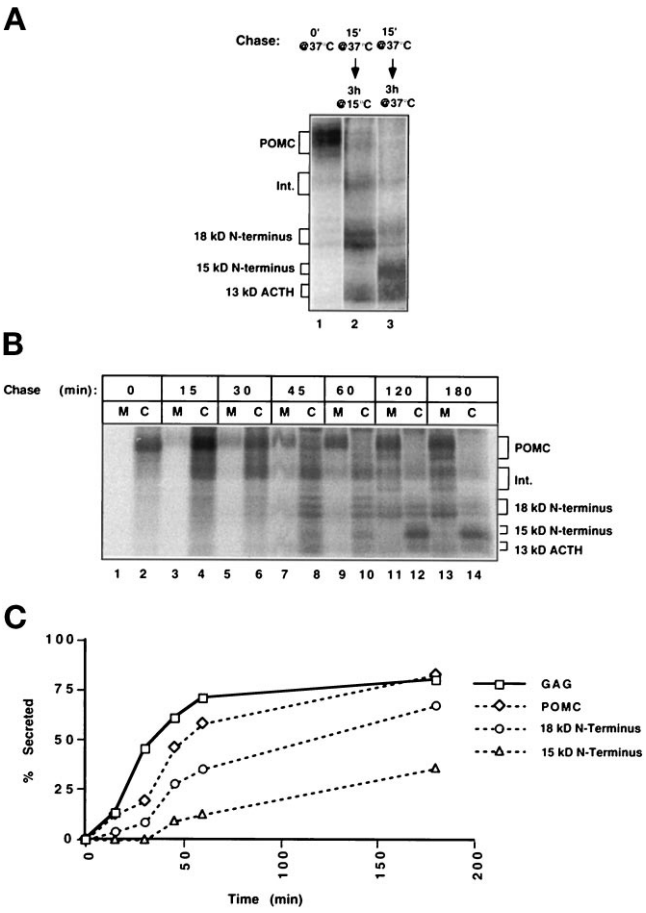

Figure 5. Cleavage products of POMC are differentially secreted and stored by AtT-20 cells. (A) The 15-kDa POMC N-terminal fragment is generated from the 18-kDa N-terminal fragment by a cleavage event that is blocked at 15°C. Cells were pulse labeled with [^{35}S]sulfate for 5 min and either extracted immediately (lane 1) or chased for 15 min at 37°C to allow POMC to proceed to the processing compartment. The cells were then incubated either at 15°C for 3 h (lane 2) or at 37°C for 3 h (lane 3). Sulfate-labeled proteins from the cell extracts were acetone precipitated and analyzed by SDS-PAGE and PhosphorImager. Incubation at 15°C blocks conversion of the 18-kDa to the 15-kDa N-terminal fragment. (B) Kinetics of unregulated secretion of all sulfated products recovered by TCA precipitation. Identical wells of cells were pulse-labeled with [^{35}S]sulfate for 5 min and then chased for the times indicated in DMEM containing bovine serum albumin. Medium (M) and cell extracts (C) were collected and processed by TCA precipitation. Material equal to approximately one-third of a 12-well was loaded onto the gel. Note the differences in the time course of production and secretion of the individual POMC-derived products. The total recovery of radioactivity was within 5% during 1- to 3-h chase. (C) Comparison of constitutive secretion of GAG chains and constitutive-like secretion of POMC products from AtT-20 cells. The secretion of POMC and the 18-kDa and the 15-kDa N-termini in B was quantitated by using the ImageQuant program (Molecular Dynamics) and normalized to the total amount of each form recovered at 180 min of chase. To determine kinetics of GAG chain secretion, cells pretreated with xyloside were pulse-labeled with [^{35}S]sulfate for 5 min and the percentage of labeled GAG chains secreted into the medium at times indicated was determined using the CPC filtration assay.

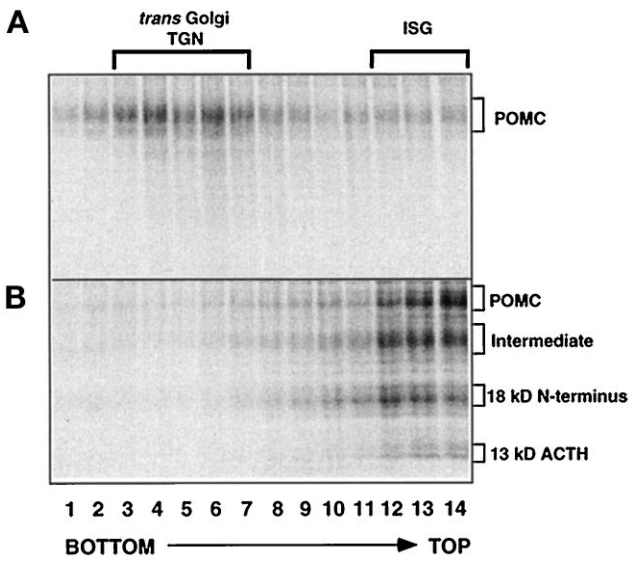

Figure 6. Velocity gradient centrifugation demonstrates that POMC is sulfated in *trans*-Golgi/TGN but is processed in vesicular fractions corresponding to ISGs. A 15-cm dish of AtT-20 cells were pulse-labeled with [^{35}S]sulfate for 5 min, and the cells were harvested either without chase (A) or after a 15-min chase at 37°C (B). A PNS was prepared and loaded on a 0.3–1.2 M sucrose gradient. Radiolabeled products were recovered from each gradient by acetone precipitation and analyzed by SDS-PAGE (on a 15% gel) and PhosphorImager.

nipulations of PNS at 4°C. These data support our conclusion that POMC sulfation occurs in the *trans*-Golgi/TGN and that the major site for proteolytic processing is the ISG.

Effect of BFA on Export from the TGN

The above analyses indicate that sulfation of POMC provides a useful tool to study post-Golgi events in the regulated secretory pathway. We next employed BFA to examine whether the various events during granule biogenesis may be uncoupled. We first demonstrate that BFA blocks export of both constitutive and regulated secretory markers from the TGN.

BFA Blocks Export of the Constitutive Secretory Marker GAG. Cells were treated with xyloside for 30 min to induce synthesis of the constitutive secretory marker GAG and pulse-labeled with [^{35}S]sulfate for 5 min. BFA (5 μg/ml) was added to the cells immediately after the pulse and the amount of labeled GAG secreted was determined (Figure 7). Secretion of GAG chains was inhibited to 18% of control level. Kinetic analysis shows that labeled GAG chains passed the BFA block with a half time of $<$10 min, suggesting that in this cell type, BFA also blocks an early step during budding of constitutive vesicles from the TGN (Miller and Moore, 1992; Dumermuth, personal communication).

BFA Abolishes Export of the Regulated Secretory Marker POMC. Likewise, BFA potently inhibits export

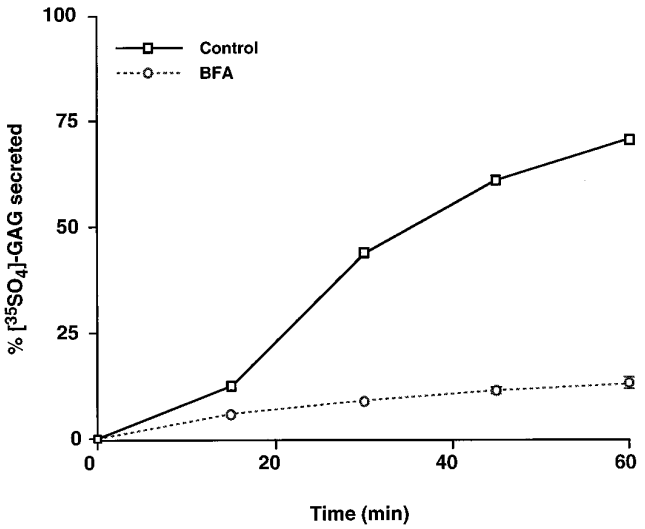

Figure 7. BFA inhibits constitutive GAG chain secretion from AtT-20 cells. Cells were treated with xyloside for 30 min and then pulse-chased with [^{35}S]sulfate for 5 min. BFA was added immediately after the pulse labeling. The cells were allowed to chase for up to 1 h. The amount of labeled GAG secreted into the medium was determined for each time point, and plotted as the percentage of total label recovered in the cell plus the medium for that time point. □, Secretion from control untreated cells; ○, secretion from BFA-treated cells.

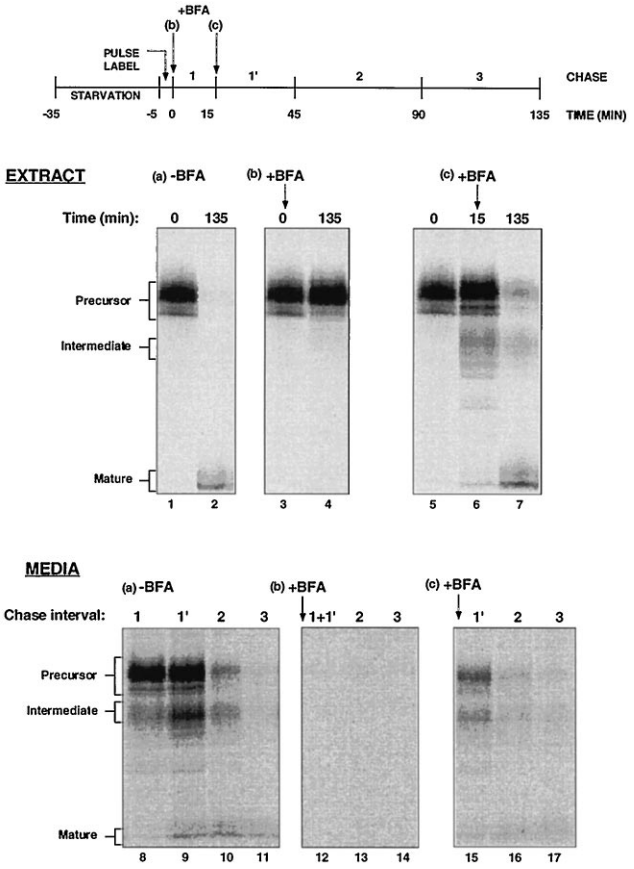

Figure 8. BFA completely blocks the exit of POMC from the sulfation compartment and partially inhibits constitutive-like secretion from the processing compartment. The basic design of this experiment is shown at the top. AtT-20 cells were pulse-labeled for 5 min with [^{35}S]sulfate. The cells were then immediately treated with 5 μg/ml BFA (condition b) or chased first for 15 min to allow the majority of labeled POMC to exit the sulfation compartment before the addition of BFA (condition c). Control cells were not treated (condition a). The cells were then chased for up to 135 min, and labeled POMC products during each chase and within the cells at the end of the chases were analyzed by immunoprecipitation, SDS-PAGE, and PhosphorImager analysis. Cell extracts were prepared at the indicated times. Lanes 1 and 2, untreated control cells; lanes 3 and 4, cells treated with BFA immediately after the pulse labeling at time 0; lanes 5–7, cells in which BFA was added after 15 min of chase. Medium samples were collected during the indicated chase intervals. Lanes 1, 0–15 min; lanes 1′, 15–45 min; lanes 2, 45–90 min; lanes 3, 90–135 min. Lanes 8–11 show secretion from untreated cells. Lanes 12–14 show that BFA completely inhibits export of POMC from the sulfation compartment. Lanes 15–17 show that BFA also reduced constitutive-like secretion from the processing compartment.

of the regulated secretory marker POMC from the sulfation compartment (Figure 8). In control cells not treated with BFA, POMC labeled during the 5-min pulse was fully converted to the 13-kDa ACTH at the end of a 135-min chase (Figure 8, lanes 1 and 2). In contrast, addition of BFA immediately after the pulse labeling (Figure 8, scheme b) completely blocked the conversion of POMC to intermediate or mature forms during the subsequent chases (Figure 8, lanes 3 and 4). Inhibition of processing was accompanied by a total block of secretion of labeled POMC products (Figure 8, compare lanes 12 -14 to lanes 8–11). Thus, these results suggest that export of both constitutive and regulated secretory markers from the TGN is abolished by BFA. The finding that BFA prevents POMC processing is consistent with the 20°C experiment that proteolytic conversion occurs after POMC exits the TGN.

Effects of BFA at the Level of ISGs

BFA Does Not Interfere with Activation of the Prohormone Processing Machinery in ISGs. To test whether BFA affects events occurring in ISGs, we first chased pulse-labeled cells for 15 min before the addition of BFA (Figure 8, scheme c); the 15-min chase was included to allow time for POMC to exit TGN and enter ISGs (Figure 6). After a 15-min chase in unlabeled medium, the majority of sulfate-labeled hormone within the cells was still in the form of unprocessed precursors, indicating that processing did not occur to a significant extent during the 15 min chase (Figure 8, lanes 5 and 6). However, addition of BFA at the 15-min chase time no longer blocked subsequent conversion of these labeled precursors to mature form (Figure 8, lane 7). Quantitation of the gel shows that <15% of POMC labeled during the pulse remained as unprocessed POMC, compared with >98% when BFA

Table 2. Summary of the effects of BFA on constitutive and constitutive-like secretion

		−BFA	+BFA	% control
GAG chains from the sulfation compartment	Medium (0–45 min)	7,167	1,312	18.3
	Extract	4,582	9,998	218.2
POMC products from the sulfation compartment	Medium (0–45 min)			
	POMC	65,202	200	0.3
	Int.	28,312	0	0
	Mature	3,421	0	0
	Medium (45–90 min)			
	POMC	4,911	260	0.7
	Int.	5,355	0	0
	Mature	2,856	0	0
	Extract			
	POMC		124,782	NA
	Mature	5,985		NA
POMC products from the processing compartment	Medium (15–45 min)			
	POMC	29,126	12,951	44.5
	Int.	8,680	4,070	46.9
	Mature	810	361	44.5
	Medium (45–90 min)			
	POMC	4,667	1,362	29.2
	Int.	7,177	1,377	19.2
	Mature	1,227	415	33.8
	Extract			
	Mature	2,147	5,338	249.6

Identical cultures of AtT-20 cells were pulse-labeled with [^{35}S]sulfate for 5 min and then chased for up to 135 min. BFA was added either immediately after the chase or to cells that had been chased for 15 min in unlabeled medium as described in Fig. 5. POMC-derived products from the medium and the cells were recovered by immunoprecipitation and analyzed by SDS-PAGE. The gels were quantitated by PhosphorImager, and the radioactivity associated with each band was expressed in arbitrary scanning unit and compared to values obtained from untreated cultures. NA indicates that values for percentage of control cannot be obtained due to unknown molar ratio for incorporation of sulfates into individual POMC forms. For GAG chains, AtT-20 cells were treated with xyloside for 30 min followed by pulse–chase labeling with [^{35}S]sulfate for 5 min. BFA was added to the cells immediately after the label, and the cells were chased for 45 min. Radioactivities associated with GAG recovered from the cells and medium were determined by the CPC/filtration assay and expressed in cpm. Int., intermediate forms.

was added immediately after the pulse (Figure 8, compare lane 7 versus lane 4). These data indicate that after a 15-min chase, >85% POMC has exited the sulfation compartment. Thus, although the formation and trafficking to ISGs is blocked by BFA, the activation of the prohormone processing machinery in ISGs does not involve BFA-sensitive trafficking events.

BFA Impairs Unregulated Release from ISGs. To determine whether the unregulated release of POMC products from ISGs is sensitive to BFA treatment, the medium samples from the above experiment were examined (Figure 8, lanes 15–17). Addition of BFA at the 15-min chase time did not completely abolish subsequent secretion of unprocessed POMC or intermediate forms, but the amount of secretion was greatly reduced (Figure 8, compare to control, lanes 9–11). A quantitative comparison of the effect of BFA on export from the TGN and on the release from ISGs is shown in Table 2. For POMC, we observed a much more severe block of export from the TGN than from ISGs by BFA. Secretion of all forms of POMC products from the sulfation compartment was blocked to <1% of control levels. By contrast, secretion of POMC products from ISGs was 44–47% of control during 15–45 min of chase, and 19–34% of control during 45–90 min of chase. The reduced unregulated release from ISGs was accompanied by an increase in the accumulation of mature ACTH within the cells (250% of control level).

ISGs Continue to Gain Buoyant Density in the Presence of BFA. The increase in buoyant density of secretory granules presumably involves fusion of ISGs followed by removal of excess membranes, a process that is likely to involve membrane budding. To test whether this process is affected by BFA, we pulse-labeled the cells for 5 min and chased for 15 min. BFA was added to the cells and the chase was continued for an additional 4 h. A PNS was prepared at the end of the chases and fractionated on a D_2O-sucrose gradient; this gradient system was used instead of the Ficoll-D_2O gradient (Figure 3) because it gave similar results but was easier to work with. Labeled POMC in ISGs prepared from cells that had been pulse-labeled and chased for 15 min was found in the light-density frac-

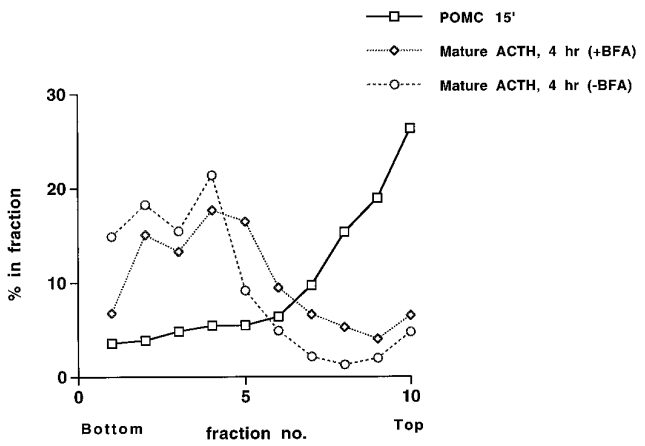

Figure 9. Condensation of secretory granules continues in the presence of BFA. AtT-20 cells were pulse-labeled with [^{35}S]sulfate for 5 min and then chased for 15 min in unlabeled medium to allow the majority of labeled POMC to exit the sulfation compartment. To study the effect of BFA on subsequent maturation of secretory granules, BFA was then added to 5 μg/ml, final concentration, and the cells were chased for an additional 4 h (with fresh BFA added after 2 h of incubation). Control cells were allowed to chase in the absence of BFA. At the end of the chases, cells were lifted from the dish and a PNS was prepared and fractionated on a D_2O-sucrose gradient. Samples from each fraction were immunoprecipitated with anti-ACTH and analyzed by SDS-PAGE and PhosphorImager. □, Distribution of unprocessed POMC after 15 min of chase before BFA addition; ○, distribution of mature ACTH after 4 h of chase in the absence of BFA; ◇, distribution of mature ACTH after 4 h of chase in the presence of BFA. The amount of labeled POMC or mature ACTH in each fraction was calculated as the percentage of the sum of total label in that form throughout the entire gradient.

tions at the top of this gradient (Figure 9), whereas fully matured granules after 4 h of chase were much denser and were recovered in the bottom half of this gradient. When BFA was added to the cells after 15 min of chase and allowed to chase in BFA for 4 h, ISGs still condensed although the density of granules appeared to be slightly lower than that of control cells. Thus, the condensation process during granule maturation appears to be largely BFA-insensitive.

DISCUSSION

In AtT-20 cells, more than 90% of radiolabeled sulfate incorporated into POMC was on N-linked carbohydrates based on the following findings. 1) Tunicamycin treatment of intact cells or endo F digestion of the immunoprecipitates drastically reduced the amount of radiolabel recovered on POMC (Figure 2). 2) The 13-kDa and the 4.5-kDa ACTH differ in glycosylation on Asn^{152}, but only the former is labeled with [^{35}S]sulfate (Figure 1). 3) Doubly glycosylated forms (the upper bands of POMC and intermediates) were labeled by [^{35}S]sulfate to higher specific activities than singly glycosylated forms (Figure 1, compare [^{35}S]methionine labeling to [^{35}S]sulfate labeling). Several lines of evidence suggests that sulfation incorporation occurs in a late Golgi compartment. First, pulse-labeled POMC is in the endo H-resistant form (Figure 2). Second, sulfation incorporation is inhibited by pretreatment of cells with monensin or BFA, which prevents trafficking of newly synthesized POMC to the *trans*-Golgi or TGN (Table 1). Finally, pulse-labeled POMC was found in membrane fractions corresponding to *trans*-Golgi/TGN (Figures 3 and 6).

Several observations support our conclusion that sulfation and processing of POMC occur in distinct compartments. Incubation of cells at 20°C (Figure 4) or in BFA (Figure 8) immediately after the pulse labeling completely blocks proteolytic cleavage of POMC. However, applying these treatments to cells after a 15-min chase does not exert the same effects on processing, suggesting that the inhibition was due to a block in transport rather than direct inhibition of prohormone convertase activities. These results suggest that labeled POMC was transported from the sulfation compartment to a processing compartment with a half time of much less than 15 min; a similar time course was reported for transport of secretogranin II from the TGN to ISGs (Tooze *et al.*, 1991). Velocity gradient analysis confirmed that during a 15-min chase, POMC moved from large membranous fractions (*trans*-Golgi/TGN) to a smaller vesicular fraction (ISGs; Figure 6). Most likely the sulfation compartment corresponds to the *trans*-Golgi/TGN, whereas the processing compartment represents ISGs. Previous electron microscopic studies have shown that processed products were detected in the dilated rim of the TGN (Schnabel *et al.*, 1989), but some unprocessed POMC was also present in mature secretory granules (Tooze *et al.*, 1987a). An interpretation that is most consistent with all of these data is that POMC processing is initiated in the dilated rim of the TGN but the majority of processing occurs in ISGs. Milgram *et al.* (1994) found that soluble peptidylglycine α-amidating monooxygenase was secreted from unstimulated AtT-20 cells with a $t_{1/2} \sim 2$ h after a methionine/cysteine pulse and suggested that this release was from ISGs. Their results are in good agreement with our kinetic analysis of sulfate-labeled POMC products ($t_{1/2} \sim 50$ min to 2 h), and the slightly faster kinetics in our system may be due to the late addition of sulfate in the secretory pathway.

BFA potently inhibits budding of constitutive vesicles from the TGN. It also impairs unregulated release from ISGs, suggesting that the mechanism underlying these two events may be similar. Several studies have also examined the effect of BFA on constitutive-like secretion from ISGs, but the results appear to differ in different systems: insulin C-peptide secretion from pancreatic β cells was not affected by BFA (Huang and Arvan, 1994), whereas constitutive-like secretion of a

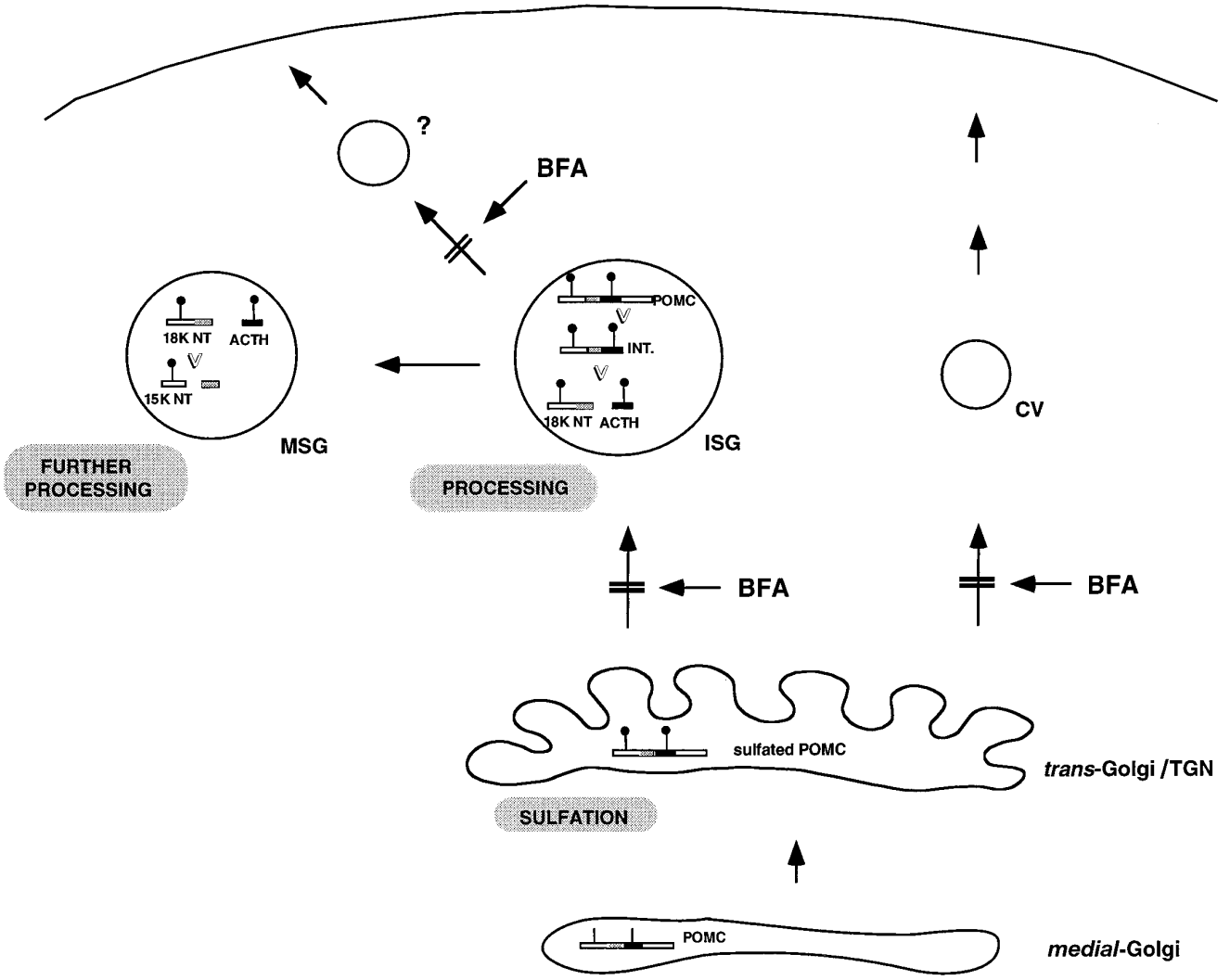

Figure 10. Working model for ACTH-granule biogenesis. POMC is transported to the *trans*-Golgi or TGN where it becomes sulfated. Budding of both constitutive secretory vesicles and nascent regulated granules is inhibited by BFA. Upon exiting the TGN, the pH of the nascent granules drops to about 5.5 to initiate proteolytic processing of POMC to yield intermediate forms, the 18-kDa N-terminal fragment, and mature ACTH. Proteolytic activation in ISGs is a BFA-insensitive process. Some unprocessed POMC, intermediate forms, and the 18-kDa N-terminal fragment exit the cells from ISGs in an unregulated manner, perhaps by incorporation into constitutive-like vesicles (question mark). This process is impaired by BFA. Maturation of ISGs is complete after 2–3 h of chase, at which time unregulated release stops and the mature granules exhibit tightly regulated state of exocytosis. This time coincides with the final cleavage of the 18-kDa N-terminal fragment, generating the 15-kDa N-terminal fragment. The latter is efficiently stored within mature secretory granules.

sulfated protein p75 from pancreatic acinar cells is inhibited by BFA (DeLisle and Bansal, 1996). Our result with AtT-20 cells is thus more in line with the findings from acinar cells than from β cells. Whether these differences reflect cell-type–specific differences or differences in the pulse–chase protocols used is presently unknown.

Tumor cells typically package hormones inefficiently. Examination of the time course of secretion of sulfated POMC products after a 5-min pulse labeling (Figure 8, lanes 8–11) shows that although some unprocessed POMC was secreted into the medium during the first 15-min chase (Figure 8, lane 8), the majority of constitutive secretion occurs during the 15–45 min of chase when labeled molecules have already reached ISGs (Figure 8, lane 9). Both unprocessed POMC and intermediate forms continued to be secreted during chase periods up to 90 min (Figure 8, lanes 9 and 10). We also observed secretion of mature ACTH that peaked at 45–90 min of chase (Figure 8, lanes 9–11). We estimate that unregulated release from ISGs accounts for at least 50% of newly synthesized hormone. In primary pancreatic β cells, more than 90% of newly synthesized proinsulin is targeted

to dense-core granules and becomes proteolytically converted to mature insulin (Rhodes and Halban, 1987; Carroll *et al.*, 1988; Kuliawat and Arvan, 1992). Our finding thus argues that at least in this AtT-20 tumor cell line, a major secretion defect is due to heightened constitutive-like secretion from ISGs.

Our model of the biogenesis of ACTH granules is shown in Figure 10. POMC is transported as the full-length precursor from the ER to the Golgi where it receives terminal glycosylation. The fully glycosylated precursor then becomes sulfated in the *trans*-Golgi/TGN. In these and earlier compartments, the ionic milieu is inappropriate for the Prohormone Convertase 1 and prevents premature proteolytic cleavage of POMC (Schmidt and Moore, 1995). Upon exit from the TGN and entry into ISGs, however, an increase in the lumenal acidity activates Prohormone Convertase 1 resulting in the sequential production of intermediate forms and mature ACTH. A significant portion of POMC precursors, intermediate forms, and the 18-kDa N-terminal fragment are released from this compartment in an unregulated manner. As ISGs mature, however, this component of unregulated release is reduced and the products contained in the final mature secretory granules are efficiently stored within the cells. This model is in accord with our kinetic data showing that the unregulated release of POMC products and other sulfated proteins occur within a time window of 2–3 h after chase and very little additional release was observed after this period (Figures 1, 5, and 8). It also explains why a late cleavage product, the 15-kDa N-terminal fragment, which is generated after 2 h, is stored much more efficiently compared with the earlier cleavage products (POMC intermediates, the 18-kDa N-terminal fragment, and the 13-kDa ACTH; Figure 5).

The unregulated release from ISGs that we observe in our study resembles the constitutive-like secretion from pancreatic cells reported previously (Kuliawat and Arvan, 1992). In that cell type, the released materials had a composition different from those retained within the cell (relatively more C-peptides than mature insulin secreted). This compositional difference suggests that the constitutive-like secretion results from vesicles that bud from ISGs rather than direct fusion of ISGs with the plasma membrane. In our study, we also observed a compositional difference in the secreted material compared with stored products, but as discussed above, the difference most likely reflects the time course of proteolytic cleavage rather than selective sorting among the contents of ISGs. What could then be the function of this constitutive-like secretion if there is no selective sorting of contents? An intriguing possibility is that budding of constitutive-like vesicles from ISGs serves an additional, and perhaps more important, function of removing membrane components of the constitutive secretory machinery that have become misincorporated into nascent granules during budding at the TGN. Budding of constitutive-like vesicles will then be a key event during the maturation of the granule membrane. An important future quest would be to define the molecular mechanisms involved and to determine how the temporal aspects of this process are controlled.

ACKNOWLEDGMENTS

We thank Dr. Y.T. Chen for providing the rab11-transfected AtT-20 cells. This work was supported by grants from the Public Health Service (GM-35239) and a grant from the Cystic Fibrosis Foundation to H.-P.M. C.J.F. was a postdoctoral Fullbright Fellow from the Ministry of Education and Science of Spain.

REFERENCES

Anderson, E.D., Van Slyke, J.K., Thulin, C.D., Jean, F., and Thomas, G. (1997). Activation of the furin endoprotease is a multiple-step process: requirements for acidification and internal propeptide cleavage. EMBO J. *18*, 1508–1518.

Bauerfeind, R., and Huttner, W.B. (1993). Biogenesis of constitutive secretory vesicles, secretory granules and synaptic vesicles. Curr. Opin. Cell Biol. *5*, 628–635.

Burgess, T.L., and Kelly, R.B. (1987). Constitutive and regulated secretion. Annu. Rev. Cell Biol. *3*, 243–293.

Cain, C.C., Sipe, D.M., and Murphy, R.F. (1989). Regulation of endocytic pH by the Na^+, K^+-ATPase in living cells. Proc. Natl. Acad. Sci. USA *86*, 544–548.

Carroll, R.J., Hammer, R.E., Chan, S.J., Swift, H.H., Rubenstein, A.H., and Steiner, D.F. (1988). A mutant human proinsulin is secreted from islets of Langerhans in increased amounts via an unregulated pathway. Proc. Natl. Acad. Sci. USA *85*, 8943–8947.

Chavez, R.A., Chen, Y.T., Schmidt, W.K., Carnell, L., and Moore, H.P.H. (1994). Expression of exogenous proteins in cells with regulated secretory pathways. Methods Cell Biol. *43*, 263–288.

Chege, N.W., and Pfeffer, S.R. (1990). Compartmentation of the Golgi complex: brefeldin-A distinguishes *trans*-Golgi cisternae from the *trans*-Golgi network. J. Cell Biol. *111*, 893–899.

Chen, Y.T., Holcomb, C., and Moore, H.P. (1993). Expression and localization of two small-molecular weight GTP-binding proteins, rab8 and rab10, by epitope tag. Proc. Natl. Acad. Sci. USA *90*, 6508–6512.

Cullen, E.I., and Mains, R.E. (1987). Biosynthesis of amidate joining peptide from proadrenocorticotropin-endorphin. Mol. Endocrinol. *1*, 583–594.

Davidson, H.W., Rhodes, C.J., and Hutton, J.C. (1988). Intraorganellar calcium and pH control proinsulin cleavage in the pancreatic beta cell via two distinct site-specific endopeptidases. Nature *333*, 93–96.

DeLisle, R.C., and Bansal, R. (1996). Brefeldin A inhibits the constitutive-like secretion of a sulfated protein in pancreatic acinar cells. Eur. J. Cell Biol. *71*, 62–71.

de Toledo, G.A., and Fernandez, J.M. (1990). Patch-clamp measurements reveal multimodal distribution of granule sizes in rat mast cells. J. Cell Biol. *110*, 1033–1039.

Dittie, A.S., Hajibagheri, N., and Tooze, S.A. (1996). The AP-1 adaptor complex binds to immature secretory granules from PC12 cells, and is regulated by ADP-ribosylation factor. J. Cell Biol. *132*, 523–536.

Fuchs, R., Schmid, S., and Mellman, I. (1989). A possible role for Na^+, K^+-ATPase in regulating ATP-dependent endosome acidification. Proc. Natl. Acad. Sci. USA *86*, 539–543.

Griffiths, G., Quinn, P., and Warren, G. (1983). Dissection of the Golgi complex I. Monensin inhibits the transport of the viral membrane proteins from medial- to *trans*-Golgi cisternae in baby hamster kidney cells infected with Semliki forest virus. J. Cell Biol. *96*, 835–850.

Grimes, M., and Kelly, R.B. (1992). Intermediates in the constitutive and regulated secretory pathways released in vitro from semi-intact cells. J. Cell Biol. *117*, 539–549.

Gumbiner, B., and Kelly, R.B. (1982). Two distinct intracellular pathways transport secretory and membrane glycoproteins to the surface of pituitary tumor cells. Cell *28*, 51–59.

Hoshina, H., Hortin, G., and Biome, I. (1982). Rat pro-opiomelanocortin contains sulfate. Science *217*, 63–64.

Huang, X.F., and Arvan, P. (1994). Formation of the insulin-containing secretory granule core occurs within immature beta-granules. J. Biol. Chem. *269*, 20838–20844.

Hutton, J.C. (1990). Subtilisin-like proteinases involved in the activation of proproteins of the eukaryotic secretory pathway. Curr. Opin. Cell Biol. *2*, 1131–1142.

Kalina, M., Elmalek, M., and Hammel, I. (1988). Intragranular processing of pro-opiomelanocortin in the intermediate cells of the rat pituitary glands. A quantitative immunocytochemical approach. Histochemistry *89*, 193–8.

Kuliawat, R., and Arvan, P. (1992). Protein targeting via the "constitutive-like" secretory pathway in isolated pancreatic islets: passive sorting in the immature granule compartment. J. Cell Biol. *118*, 521–529.

Kuliawat, R., and Arvan, P. (1994). Distinct molecular mechanisms for protein sorting within immature secretory granules of pancreatic beta-cells. J. Cell Biol. *126*, 77–86.

Lew, S., Hammel, I., and Galli, S.J. (1994). Cytoplasmic granule formation in mouse pancreatic acinar cells. Evidence for formation of immature granules (condensing vacuoles) by aggregation and fusion of progranules of unit size, and for reductions in membrane surface area and immature granule volume during granule maturation. Cell Tissue Res. *278*, 327–36.

Lindberg, I. (1991). The new eukaryotic precursor processing proteinases. Mol. Endocrinol. *5*, 1361–1365.

Mains, R.E., and Eipper, B.A. (1978). Coordinate synthesis of corticotropins and endorphins by mouse pituitary tumor cells. J. Biol. Chem. *253(3)*, 651–655.

Matlin, K.S., and Simons, K. (1983). Reduced temperature prevents transfer of a membrane glycoprotein to the cell surface but does not prevent terminal glycosylation. Cell *34*, 233–243.

Meko, J., and Norton, J. (1995). Management of patients with Zollinger-Ellison syndrome. Annu. Rev. Med. *46*, 395–411.

Milgram, S.L., Eipper, B.A., and Mains, R.E. (1994). Differential trafficking of soluble and integral membrane secretory granule-associated proteins. J. Cell Biol. *124*, 33–41.

Milgram, S.L., and Mains, R.E. (1994). Differential effects of temperature blockade on the proteolytic processing of three secretory granule-associated proteins. J. Cell Sci. *107*, 737–745.

Miller, S.G., and Moore, H.-P.H. (1992). Movement from the *trans*-Golgi network to the cell surface in semi-intact cells. Methods Enzymol. *219*, 234–248.

Modlin, I., Lewis, J., Ahlman, J., Bilchik, A., and Kumar, R. (1993). Management of unresectable malignant endocrine tumors of the pancreas. Surgery, Gynecology, and Obstetrics *176*, 507–518.

Moore, H.-P.H., Carnell, L., Chavez, R.A., Chen, Y.-T., Hwang, A., Miller, S.G., Yoon, Y.-A., and Yu, H., Ed. (1993). Regulated and constitutive secretion studied in vitro: control by G proteins at multiple levels. In: Handbook of Experimental Pharmacology, "GTPase in Biology," ed. B. Dickey and L. Birnbaumer, Berlin: Springer-Verlag, Vol. 108/1, Chapter 33, 507–528.

Moore, H.-P.H., Gumbiner, B., and Kelly, R.B. (1983a). A subclass of proteins and sulfated macromolecules secreted by AtT-20 (mouse pituitary tumor) cells is sorted with adrenocorticotropin into dense secretory granules. J. Cell Biol. *97*, 810–817.

Moore, H.-P.H., and Kelly, R.B. (1985). Secretory protein targeting in a pituitary cell line: differential transport of foreign secretory proteins to distinct secretory pathways. J. Cell Biol. *101*, 1773–1781.

Moore, H.-P.H., and Kelly, R.B. (1986). Rerouting of a secretory protein by fusion with human growth hormone sequences. Nature *321*, 443–446.

Moore, H.-P.H., Walker, M., Lee, F., and Kelly, R.B. (1983b). Expressing a human proinsulin cDNA in a mouse ACTH secretory cell. Intracellular storage, proteolytic processing and secretion on stimulation. Cell *35*, 531–538.

Ngsee, J.K., Fleming, A.M., and Scheller, R.H. (1993). A rab protein regulates the localization of secretory granules in AtT-20 cells. Mol. Biol. Cell *4*, 747–756.

Orci, L., Halban, P., Perrelet, A., Amherdt, M., Ravazzola, M., and Anderson, R.G. (1994). pH-independent and -dependent cleavage of proinsulin in the same secretory vesicle. J. Cell Biol. *126*, 1149–1156.

Orci, L., Ravazzola, M., Amherdt, M., Perrelet, A., Powell, S., Quinn, D., and Moore, H.-P.H. (1987). The *trans*-most cisternae of the Golgi complex: a compartment for sorting of secretory and plasma membrane proteins. Cell *51*, 1039–1051.

Orth, D. (1995). Cushing's syndrome. New Engl. J. Med. *332*, 791–803.

Reaves, B.J., Van Italli, C.M., Moore, H.-P.H., and Dannies, P.S. (1990). Prolactin and insulin are targeted to the regulated pathway in GH4C1 cells but their storage is differentially regulated. Mol. Endocrinol. *4*, 1017–1026.

Rhodes, C.J., and Halban, P. (1987). Newly synthesized proinsulin/insulin and stored insulin are released from pancreatic B cells predominantly via a regulated, rather than a constitutive, pathway. J. Cell Biol. *105*, 145–153.

Schmidt, W.K., and Moore, H.-P.H. (1995). Ionic milieu controls the compartment-specific activation of pro-opiomelanocortin processing in AtT-20 cells. Mol. Biol. Cell *6*, 1271–1285.

Schnabel, E., Mains, R.E., and Farquhar, M.G. (1989). Proteolytic processing of pro-ACTH endorphin begins in the Golgi complex of pituitary corticotropes and AtT-20 cells. Mol. Endocrinol. *3*, 1223–1235.

Seidah, N.G., Day, R., and Chretien, M. (1993). The family of prohormone and pro-protein convertases. Biochem. Soc. Trans. *21*, 685–691.

Steiner, D.F., Smeekens, S.P., Ohagi, S., and Chan, S.J. (1992). The new enzymology of precursor processing endoproteases. J. Biol. Chem. *267*, 23435–23438.

Thomas, L., Leduc, R., Smeekens, S.P., Steiner, D.F., and Thomas, G. (1991). Kex2-like endoproteases PC2 and PC3 accurately cleave a model prohormone in mammalian cells: evidence for a common core of neuroendocrine processing enzymes. Proc. Natl. Acad. Sci. USA *88*, 5297–5301.

Tooze, J., Hollinshead, M., Frank, R., and Burke, B. (1987a). An antibody specific for an endoproteolytic cleavage site provides evidence that pro-opiomelanocortin is packaged into secretory granules in AtT20 cells before its cleavage. J. Cell Biol. *105*, 155–162.

Tooze, J., Tooze, S.A., and Fuller, S.D. (1987b). Sorting of progeny coronavirus from condensed secretory proteins at the exit from the *trans*-Golgi network of AtT-20 cells. J. Cell Biol. *105*, 1215–1226.

Tooze, S.A., Flatmark, R., Tooze, J., and Huttner, W.B. (1991). Characterization of the immature secretory granule, an intermediate in granule biogenesis. J. Cell Biol. *115*, 1491–1503.

Tooze, S.A., and Huttner, W.B. (1990). Cell-free protein sorting to the regulated and constitutive secretory pathways. Cell *60*, 837–847.

Urbe, S., Huber, L.A., Zerial, M., Tooze, S.A., and Parton, R.G. (1993). Rab11, a small GTPase associated with both constitutive and regulated secretory pathways in PC12 cells. FEBS Lett. *334*, 175–182.

von Zastrow, M., and Castle, J.D. (1987). Protein sorting among two distinct export pathways occurs from the content of maturing exocrine storage granules. J. Cell Biol. *105*, 2675–84.

Xu, H., and Shields, D. (1994). Prosomatostatin processing in permeabilized cells. Endoproteolytic cleavage is mediated by a vacuolar ATPase that generates an acidic pH in the *trans*-Golgi network. J. Biol. Chem. *269*, 22875–22881.